Journal of Magnetic Resonance 193 (2008) 94–101

Contents lists available at ScienceDirect

Journal of Magnetic Resonance

journal homepage: www.elsevier.com/locate/jmr

High-resolution NMR spectra in inhomogeneous fields utilizing the CRAZED sequence without coherence selection gradients

Congbo Cai [a], Yanqin Lin [a], Shuhui Cai [a], Zhong Chen [a,*], Jianhui Zhong [b]

[a] Departments of Physics and Communications Engineering, State Key Laboratory for Physical Chemistry of Solid Surface, Xiamen University, Siming South Road, Xiamen, Fujian 361005, China
[b] Department of Radiology, University of Rochester, Rochester, NY 14642, USA

ARTICLE INFO

Article history:
Received 9 February 2008
Available online 22 April 2008

Keywords:
High-resolution spectra
Intermolecular multiple-quantum coherences
Inhomogeneous fields
Dipolar correlation distance
Coherence selection gradients

ABSTRACT

Coherence selection gradients have been considered as indispensable for high-resolution NMR spectroscopy in inhomogeneous fields utilizing the CRAZED-type sequences. However, our experimental results demonstrate that these gradients can be omitted if an appropriate phase cycling is applied. The measured linewidth of reconstructing 1D high-resolution spectral peaks does not depend on the dipolar correlation distance determined by the coherence selection gradients, but is only affected by diffusion and T_2 relaxation. This finding suggests the need to reconsider the mechanism for the iMQC-based high-resolution spectroscopy.

1. Introduction

Intermolecular multiple-quantum coherences (iMQCs) possess numerous interesting properties [1–3]. Since the early 1990s, Warren and co-workers have presented a series of seminal papers to characterize iMQCs in highly polarized nuclear spin systems such as water [4–6]. The pulse sequences for creating iMQCs, mostly based on COSY Revamped with Asymmetric *Z*-gradient Echo Detection (CRAZED), usually contain gradient pulses that modulate the transverse magnetization into a helical structure [7]. When the ratio of the coherence selection gradient (CSG) areas before and after the second RF pulse in the CRAZED sequence is $G\delta$:$nG\delta$ (where G and δ are the amplitude and duration of the first CSG pulse), the n order iMQC signals are observed [8,9].

IMQCs arise primarily from dipole–dipole interactions of nuclei within a macroscopic separation, called dipolar correlation distance r_d, which is inversely proportional to the area of the first CSG pulse [10,11]. One of the attractive properties of iMQCs is that they can be used to encode structural information over intermediate length scales, whether it is contained inside an imaging voxel or buried in the bulk material [12]. This unique property has been used to provide distance-selected contrast sensitive to differences in resonance frequency and magnetization density [13,14]. It can also be utilized for *in vivo* high-resolution NMR spectra [15].

In vivo NMR spectroscopy is challenging in the presence of magnetic field inhomogeneity induced by differences in magnetic susceptibility e.g. between tissues and air [16]. This inhomogeneity results in broad spectral peaks and hence low spectral resolution [17]. Besides recent improvements in shimming techniques [18,19], many methods have been developed to extract high-resolution NMR information from the spectra acquired in inhomogeneous magnetic fields. Blümich and co-workers developed a unilateral and mobile NMR sensor for high-resolution NMR spectra at low magnetic field strengths [20,21]. More recently, a method for obtaining high-resolution spectra of a rat brain *in vivo* was proposed via detection of intramolecular zero-quantum coherences [17]. Although these techniques can partially remove inhomogeneous broadening, they cannot provide correct multiplet patterns and relative peak areas. IMQC methods have been shown to be able to recover high-resolution NMR spectra from inhomogeneous fields [22–27]. Unlike a conventional spectrum with its linewidth determined by the absolute homogeneity of a magnetic field across the whole sample, the linewidth of a high-resolution 1D spectrum based on iMQC methods is generally thought to depend only on the relative homogeneity of a magnetic field over the dipolar correlation distance $r_d = \pi/\gamma G\delta$ [28,10], where γ is the magnetogyric ratio of the nucleus. Therefore, to obtain an iMQC high-resolution spectrum, CSGs have always been included in all the iMQC pulse sequences so far. The CSG is used to encode the distant dipolar field (DDF) and select signals with the expected coherence order and within the defined spatial regions. However, our work shown below demonstrates that the CSG is not necessary for an iMQC

* Corresponding author. Fax: +86 592 2189426.
E-mail address: chenz@xmu.edu.cn (Z. Chen).

1090-7807/$ - see front matter © 2008 Elsevier Inc. All rights reserved.
doi:10.1016/j.jmr.2008.04.028

high-resolution spectrum in an inhomogeneous field if an appropriate phase cycle scheme is used.

2. Theories and methods

There are two superficially quite different frameworks for analyzing the long-range dipolar interactions in NMR spectroscopy: classical treatment [29–31] and quantum formalism [4,6]. In the two frameworks, the underlying spin physics of related experiments has been described in terms of DDF formalism, which results from integrated effects of dipolar interactions [32,33], or equivalently, in terms of iMQCs [5,6,26]. In the current work, DDF theory [32–34] is employed for theoretical deduction. For simplification, we consider a homogeneous liquid mixture consisting of two single spin-1/2 systems of S and I components. It is assumed that I spin (corresponding to solvent) is abundant, and S spin (corresponding to solute) is dilute. ω_I and ω_S are the frequency offsets of spins I and S, respectively, in the rotating frame in the absence of field inhomogeneity. The effects of radiation damping and T_1 relaxation are ignored. The background field is assumed to be only inhomogeneous along the Z axis, and the CSG is also along the Z axis. $\Delta B(z)$ is the field inhomogeneity at position z. If the magnetization is fully modulated and varies only in one direction, the dipolar field is localized and an exact theoretical expression for the iMQC signal can be deduced [35].

The IDEAL (Intermolecular Dipolar-interaction Enhanced All Lines) pulse sequence, a modified version of the CRAZED sequence, was used to select intermolecular double-quantum coherence (iDQC) signal [22]. When the second gradient pulse of the original IDEAL sequence is set to zero, the sequence can be used to produce intermolecular zero-quantum coherence (iZQC) signal (shown in Fig. 1). The first and last RF pulses are non-selective, and the second RF pulse is selective for solvent. The expression for the signal from S spin is deduced to be:

$$M_S^{\pm}(z,t_2) = M_S e^{i(\pi/2-\alpha_1-\omega_S t_1+\omega_S t_2+\beta)} e^{-(t_1/T_2^S+(2\Delta+t_2)/T_2^{*S})} \times \sum_{m=-\infty}^{\infty} i^m J_m\left(\frac{2}{3}\gamma\mu_0 M_I(2\Delta+t_2)e^{-t_1/T_2^I}\right) \times e^{i[m\alpha_1+m\omega_I t_1+m\gamma Gz\delta+m\gamma\Delta B(z)t_1-m\alpha_2-\gamma Gz\delta-\gamma\Delta B(z)t_1+\gamma\Delta B(z)t_2]}, \quad (1)$$

where μ_0 is vacuum magnetic permeability; α_1, α_2 and β are the phases of the first RF pulse, the second RF pulse and the receiver, respectively. T_2^* includes the effects of T_2 relaxation and diffusion during the evolution time Δ and t_2. J_m is the m order Bessel function. M_S and M_I are the equilibrium magnetization densities of spins S and I, respectively. For iZQCs, a four-step phase cycling scheme with the phases of the first RF pulse (x,x,y,y), the second RF pulse $(x,-x,x,-x)$ and the receiver $(x,-x,x,-x)$ is employed. After the four-step phase cycling is taken and the high order terms ($|m| \geqslant 3$) are ignored, Eq. (1) becomes:

$$M_S^{\pm}(z,t_2) = -4M_S e^{-(t_1/T_2^S+(2\Delta+t_2)/T_2^{*S})} J_1\left(\frac{2}{3}\gamma\mu_0 M_I(2\Delta+t_2)e^{-t_1/T_2^I}\right) \times e^{i[(\omega_I-\omega_S)t_1+\omega_S t_2+\gamma\Delta B(z)t_2]}. \quad (2)$$

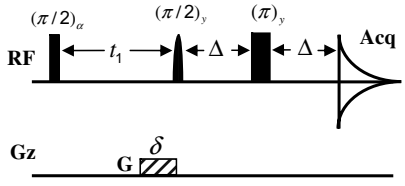

Fig. 1. IDEAL pulse sequence (a modified CRAZED) used in this paper. In the simulation, δ = 1.2 ms and Δ = 60.0 ms.

Eq. (2) shows that the intermolecular cross-peak appears at $(\omega_S-\omega_I,\omega_S)$, and the inhomogeneous field is refocused in the indirect dimension. It also indicates that the signal is of the iZQCs in origin.

It should be noted that although the CSG term appears in Eq. (1), it disappears in Eq. (2). This suggests that the CSG can be dispensed if an appropriate phase cycling scheme is employed.

Similarly, for iDQCs, when a four-step phase cycling scheme with the phases of the first RF pulse $(x,-x,y,-y)$ and the receiver $(x,x,-x,-x)$ is employed, the following expression can be obtained:

$$M_S^{\pm}(z,t_2) = 4M_S e^{-(t_1/T_2^S+(2\Delta+t_2)/T_2^{*S})} J_{-1}\left(\frac{2}{3}\gamma\mu_0 M_I(2\Delta+t_2)e^{-t_1/T_2^I}\right) \times e^{i[-(\omega_S+\omega_I)t_1+\omega_S t_2-2\gamma\Delta B(z)t_1+\gamma\Delta B(z)t_2]}. \quad (3)$$

Eq. (3) shows that the iDQC signal has similar properties as the iZQC signal. The CSG is also dispensable if an appropriate phase cycling scheme is applied. In the following, we will limit our discussion to iZQCs.

3. Experiments and simulations

All ^{1}H NMR experiments were performed at 298 K on a 500 MHz spectrometer (Varian NMR System, USA) using a 5 mm indirect detection probe with three-dimension gradient coils. The sample was a solution of methyl ethyl ketone in cyclohexane. The pulse sequence used is shown in Fig. 1. The gradient duration δ was 1.2 ms and the strength was varied from zero to 0.13 T/m. The inhomogeneous fields were created by deliberately deshimming some specific shimming coils to produce a linewidth of about 200 Hz. The spectral width of the F1 dimension was 1200 Hz in 512 increments, and was 1600 Hz for the F2 dimension. The acquisition time t_2 was 1.0 s. The signal was zero filled to 4096 × 4096 before a regular FFT process.

To compare with the experimental results, we also performed numerical simulations since exact theoretical analysis is intractable for differences between iZQC signals obtained with and without CSGs, especially when the inhomogeneous field and the CSGs are not along the same direction. All simulations were carried out using the software package, SPROM, developed by our group [36,37]. To reduce computation time, a simplified sample with only two isolated spin systems was used, denoted as I (solvent) and S (solute). Following parameters were used: for the I spin system, the chemical shift ω_I = 0 Hz, diffusion rate $D^I = 2.0 \times 10^{-9}$ m^2/s, equilibrium magnetization density $M_0^I = 0.03$ A/m, and transverse relaxation time $T_2^I = 0.5$ s; for the S spin system, the chemical shift ω_S = 375 Hz, and the other parameters are the same as the spin system I. Other simulation parameters were close to the experimental parameters, including the inhomogeneous field strength and the size of the sample. Because the RF pulse flip angles in the experiments were not completely ideal, they were deliberately deviated from the ideal ones by about 5% to make the simulation results better matched to the experimental ones. 512 points were sampled in the direct dimension (F2) with 512 increments in the indirect dimension (F1). Both dimensions were zero-filled to 4096 points. In a general case, it took about 24 h of CPU time on a PC computer (Intel E6750, 2 Gb memories) to obtain a 2D spectrum. When the inhomogeneous field and the CSG was along the same direction, the CPU time for a simulation was reduced to several minutes.

The conventional 1D NMR experimental spectra for the sample are shown in Fig. 2. Fig. 2a is for the case with a homogeneous field, while Fig. 2b–d is for the cases with different kinds of inhomogeneous fields: linear along the XY plane, non-linear along the XY plane, and liner along the Z axis, respectively. The linear inhomogeneous field along the XY plane was produced by deshimming the $X1$ and $Y1$ coils, the non-linear inhomogeneous field along the XY

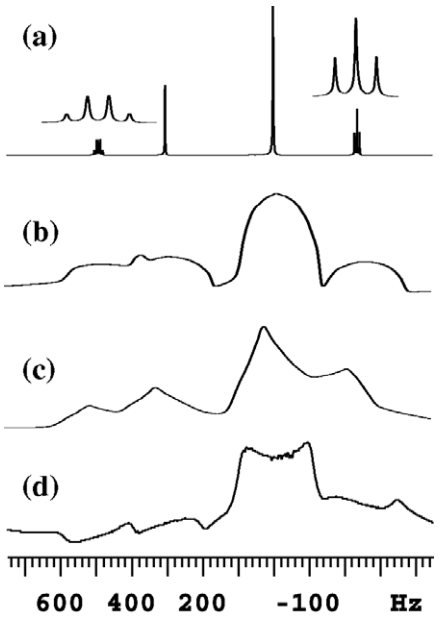

Fig. 2. Conventional 1D NMR spectra under different kinds of inhomogeneous fields. (a) Homogeneous field, (b) about 200 Hz linewidth linear along the *XY* plane, (c) about 200 Hz linewidth non-linear along the *XY* plane, and (d) about 200 Hz linewidth linear along the *Z* axis.

plane was produced by deshimming the *XY*, *X*2*Y*2, *X*1 and *Y*1 coils, and the linear inhomogeneous field along the *Z* axis was achieved by deshimming the *Z*1 coil. In practice, deshimming the *XY* and *X*2*Y*2 coils in a routine spectrometer can at most generate an inhomogeneous field with about 40 Hz linewidth. Therefore, for the non-linear inhomogeneity with 200 Hz linewidth, the linear terms are still dominant in usual cases. One can see that the conventional 1D NMR spectra acquired in these different kinds of inhomogeneous fields provide little information about chemical shifts and *J* couplings. The peaks with different chemical shifts overlap greatly. In addition, the linear and non-linear inhomogeneous fields along the *XY* plane give quite different 1D spectra. In the simulations, the linear inhomogeneous field was along the *Z* axis and *X* axis, respectively. The non-linear inhomogeneous field was only along the *X* axis with the following relationship: $B_1(x) = a(x + x^3)$, where $B_1(x)$ is the background inhomogeneous field at position *x*, and *a* is a constant depending on the inhomogeneous linewidth.

The 2D iZQC spectra under the corresponding inhomogeneous fields are shown in Fig. 3. The spectra shown in the left side of Fig. 3a, c and e are obtained with a gradient strength $G = 0.09$ T/m of the CSG, while the spectra shown in the right side of Fig. 3b, d and f are obtained without any CSGs. Although CSGs were not used for the spectra shown in the right side of Fig. 3, the observed signal still came from iZQCs, as can be deduced from the coherence transfer pathway. Therefore the method is still iZQC-related. All these spectra show that iZQCs can give high-resolution spectra in the indirect dimension under highly inhomogeneous fields, independent of whether a CSG is applied or not. For the singlet from the methyl group of methyl ethyl ketone, the linewidth under the inhomogeneous field linear along the *XY* plane was decreased from about 200–16 Hz with $G = 0.09$ T/m, and to 9 Hz with $G = 0$ T/m; the linewidth under the inhomogeneous field non-linear along the *XY* plane was decreased from about 200–18 Hz with $G = 0.09$ T/m, and to 10 Hz with $G = 0$ T/m; the linewidth under the inhomogeneous field linear along the *Z* axis was decreased from about 200 Hz to 4.5 Hz with $G = 0.09$ T/m, and to 4.0 Hz with $G = 0$ T/m. Thus the IDEAL pulse sequence without any CSGs can produce high-resolution spectra in inhomogeneous fields if appropriate phase cycling is applied. In the 1D projections of the peaks from Fig. 3, spectral features of chemical shifts and scalar couplings can be well resolved. Furthermore, the iZQC spectra obtained without CSGs show better resolution compared to the spectra obtained with $G = 0.09$ T/m. The main reasons may be because that CSG introduces additional diffusion decay and interacts with the inhomogeneous field. Discussion in more details will be given in the next section.

The dependence of the experimental iZQC linewidth in the indirect dimension on the strength of the CSG is illustrated in Fig. 4a. For simplicity, only the linewidth of the singlet from the methyl group of methyl ethyl ketone is shown. It can be seen that the variation trends are similar for the linear and non-linear inhomogeneous fields along the *XY* plane. For the linear inhomogeneous field along the *XY* plane, the linewidth reaches a maximal value of about 24 Hz when the CSG is $G = 0.03$ T/m. For the non-linear inhomogeneous field along the *XY* plane, a maximal linewidth of about 30 Hz occurs at $G = 0.05$ T/m. The linewidth is minimal when there is no CSG for both the linear and non-linear inhomogeneous fields along the *XY* plane. Different features appear when the inhomogeneous field is along the *Z* axis. First, the linewidths from the inhomogeneous field along the *Z* axis are between 4.0 and 4.7 Hz, much smaller than the linewidths obtained in the cases when the inhomogeneous field is along the *XY* plane. Secondly, the linewidths obtained from different *G* are similar to each other. The simulation results shown in Fig. 4b are deemed in accordance with the experimental results, considering that some experimental conditions are not duplicated completely in the simulation.

Fig. 5 shows the simulation results of variations of *S* spin signal intensity with the evolution time t_1 under different CSGs. Fig. 5a is for the linear inhomogeneous field along the *XY* plane, and Fig. 5b is for the linear inhomogeneous field along the *Z* axis. Fig. 5 demonstrates that the signal intensity in the linear inhomogeneous field along the *XY* plane does not monotonously decrease with increasing evolution time t_1 for some small CSGs, while it monotonously decreases in the linear inhomogeneous field along the *Z* axis.

The experimental 2D iZQC spectra with a CSG strength $G = 0.03$ T/m along *Z* axis under different kinds of inhomogeneous fields are shown in Fig. 6. When the inhomogeneous field is along the *XY* plane, the singlet B is strongly distorted, and the peaks A and C also deviate from the conventional triplet and quadruplet. However, when the inhomogeneous field is along the *Z* axis, the conventional peak splitting pattern is well reserved. For comparison, Fig. 7 shows the corresponding simulation results, which have similar characteristics as shown in Fig. 6. When the inhomogeneous field is along the *XY* plane, the singlet *S* is distorted. However, when the inhomogeneous field is along the *Z* axis, the *S* peak remains a singlet.

4. Discussion

The ability of iMQCs in narrowing linewidth under inhomogeneous fields has been thought to be due to the relative homogeneity within the dipolar correlation distance determined by the CSG. However, the results presented in this work demonstrate that the ability of iZQC method in reconstructing 1D high-resolution NMR spectra in the presence of inhomogeneous fields does not depend on the use of the CSG. CSGs are not absolutely needed for iMQC high-resolution spectra. Therefore, the source of iMQC high-resolution spectra may need to reconsider to some extent.

In fact, either an inhomogeneous background field or a CSG can produce modulation of magnetization, which yields a DDF. Without a CSG, the dipolar correlation distance must be defined in a different way. For simplicity, let us assume that the background

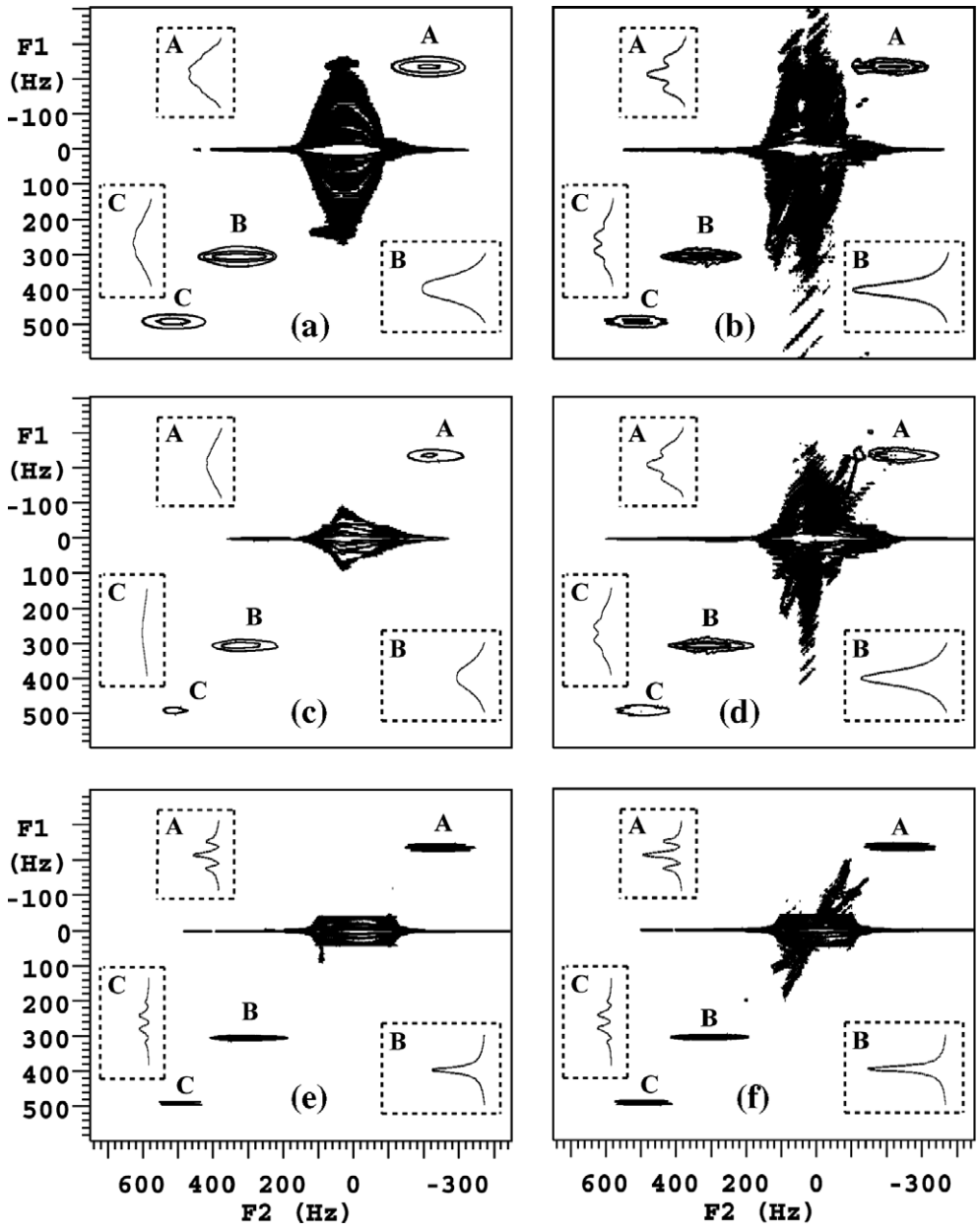

Fig. 3. Experimental 2D iZQC spectra in inhomogeneous fields with 200 Hz linewidth, generated by different settings of shimming gradients. (a) Linear along the *XY* plane and $G = 0.09$ T/m, (b) linear along the *XY* plane and $G = 0.0$ T/m, (c) non-linear along the *XY* plane and $G = 0.09$ T/m, (d) non-linear along the *XY* plane and $G = 0.0$ T/m, (e) linear along the *Z* axis and $G = 0.09$ T/m, and (f) linear along the *Z* axis and $G = 0.0$ T/m. A four-step phase cycling was applied. The regions of the solute peaks were expanded.

inhomogeneous field is linear along the *Z* axis. Similar to the CSG method, the corresponding dipolar correlation distance caused by the linear background field can be defined as

$$r = \frac{\pi}{\gamma g T}, \tag{4}$$

where T is the maximal t_1 value in the indirect dimension, and g is the strength of the background field gradient. It means that when the inhomogeneity of a background field is large at a place, the related correlation distance will be small. So the background inhomogeneous field can always be thought to be relative homogeneous inside the correlation distance thus defined. Because t_1 is increased from 0 to T during the acquisition of a 2D spectrum, r can be thought as the minimal dipolar correlation distance that can be reached. The linewidth Δf within the dipolar correlation distance r is then given by

$$\Delta f = \frac{\gamma g r}{2\pi} = \frac{1}{2T}. \tag{5}$$

If the effects of diffusion attenuation and T_2 relaxation are ignored, the linewidth of a high-resolution spectrum will only be restricted by Eq. (5). According to the discrete Fourier transform theory, the maximal spectral resolution in the indirect dimension is $1/T$ in this situation. Therefore, the ability of iMQC method in achieving high-resolution spectra from inhomogeneous fields may not be restricted by the background field inhomogeneity, but only by T and signal attenuation factors caused by relaxation and diffusion. This is important for the application of iMQCs in localized high-resolution magnetic resonance spectroscopy, where the field fluctuation due to susceptibility change at the interfaces of air, tissue, and bone is rapid over short distances [38].

As we can see, Eq. (5) does not include any terms related to inhomogeneous linewidth. It means that although our experi-

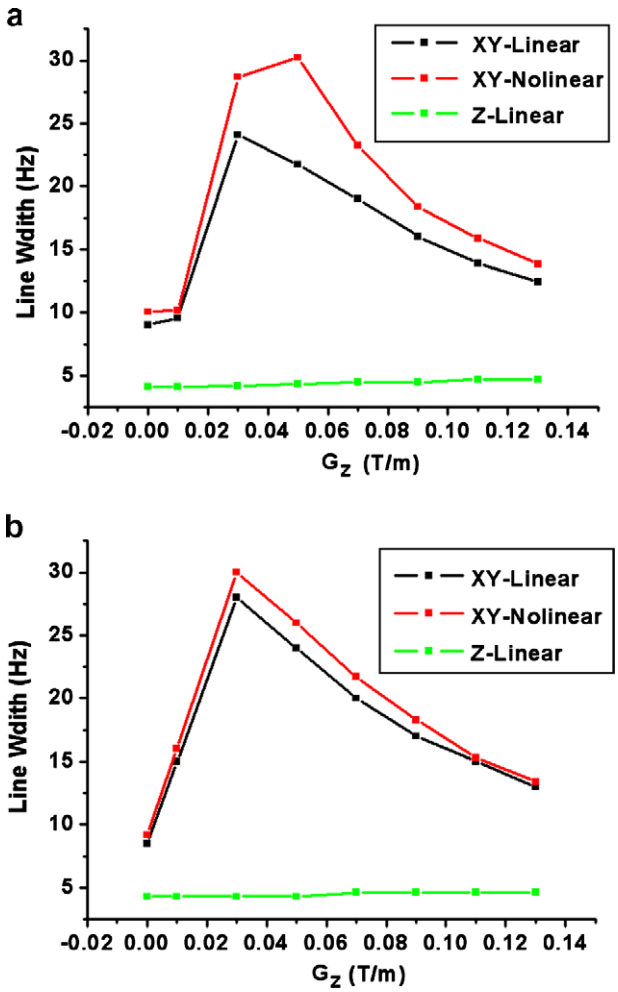

Fig. 4. Variations of iZQC linewidth with CSG strength. (a) Experimental results, and (b) simulation results.

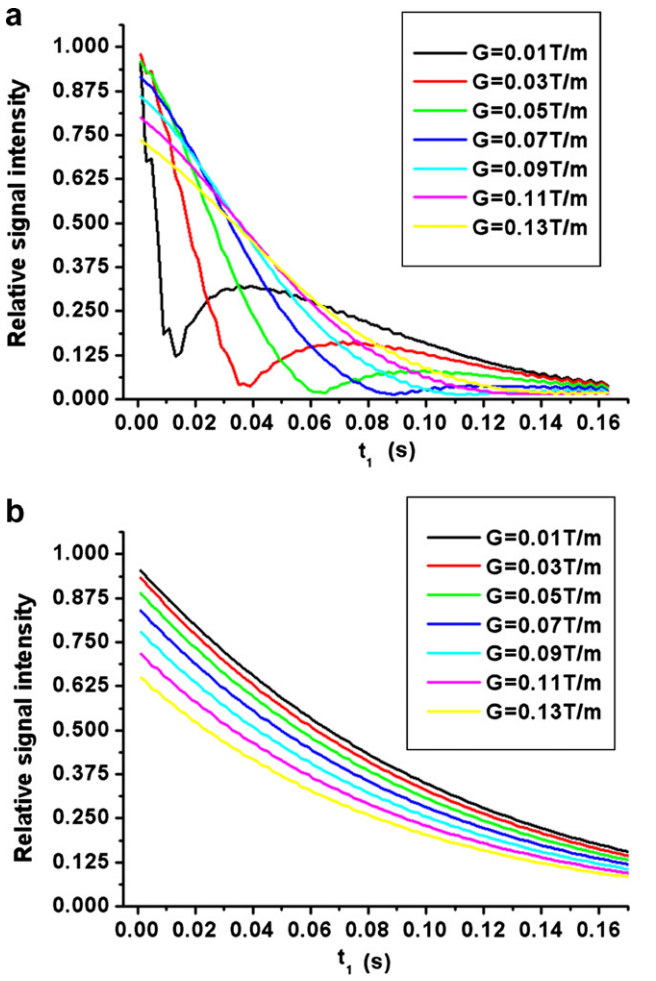

Fig. 5. Variations of S signal intensity with evolution time t_1 at different CSG in different kinds of inhomogeneous fields. (a) Linear along the XY plane, and (b) linear along the Z axis.

ments and simulations were performed under the inhomogeneous field of 200 Hz linewidth, the results are valid for inhomogeneous fields of more general form in principle. In the case of a large inhomogeneous field, signal decay due to diffusion and T_2 relaxation is very fast, so it is difficult to reconstruct 1D high-resolution spectra with proper signal-to-noise ratio. On the other hand, since none of the sample can be perfectly homogeneous, the DDF always exists. For a sample with a slightly inhomogeneous field (e.g. ~1 Hz linewidth), our experimental and simulated results demonstrate that iZQC signals can still be obtained without a CSG. Besides the iZQC cross-peaks, it is not surprising that some cross-peaks originating from conventional single-quantum coherences (SQCs) appear at different positions in the 2D spectrum (data not shown).

Although Eq. (5) was deduced for the linear inhomogeneous field, it may still be valid for other types of inhomogeneous fields such as the one in non-linear form illustrated in Fig. 3d and 4. It is noted that the internal inhomogeneous field is still dominantly linear along certain direction (not randomly distributed) in our experiments and simulations. In general, since the DDF under a non-linear inhomogeneous field is not localized, a general theoretical analysis is quite difficult. Another noticeable precaution is that the non-linear inhomogeneous fields studied in this paper are non-linear in the macroscale while they are approximately linear in the microscale. If the magnetic field fluctuation is rapid over a short distance such as at the interface of different tissues, the inhomogeneous field is non-linear in the microscale. For this situation, further theoretical and experimental work is required.

Fig. 4 shows that when the strength of a CSG is between 0.03 and 0.05 T/m, the linewidth has a maximal value under the inhomogeneous field along the XY plane. This is in contrast to the case when the inhomogeneous field is along the Z axis, where the linewidth increases monotonously and slowly with the increase of the CSG strength. The broadening of linewidth can be explained by the increase of signal attenuation (Fig. 5) from diffusion effects due to the increase of the CSG strength. Because the diameter of sample in an NMR tube is much smaller than the length of sample, the background gradient is much stronger for the inhomogeneous field along the XY plane than that along the Z axis at the same inhomogeneous linewidth, thus the diffusion effect along the XY plane is much stronger. The diffusion attenuation factor for the inhomogeneous field along the XY plane is calculated to be about 12 times of that for the inhomogeneous field along the Z axis with the same inhomogeneous linewidth. This is the main reason why the iZQC spectra obtain in the inhomogeneous field along the Z axis have much narrower peaks than those obtained in the inhomogeneous field along the XY plane under the same inhomogeneity. This also explains why the signal intensity decays quickly with the increasing of evolution time t_1 when the inhomogeneous field is along the XY plane, while it is far slower when the inhomogeneous field is along the Z axis (Fig. 5).

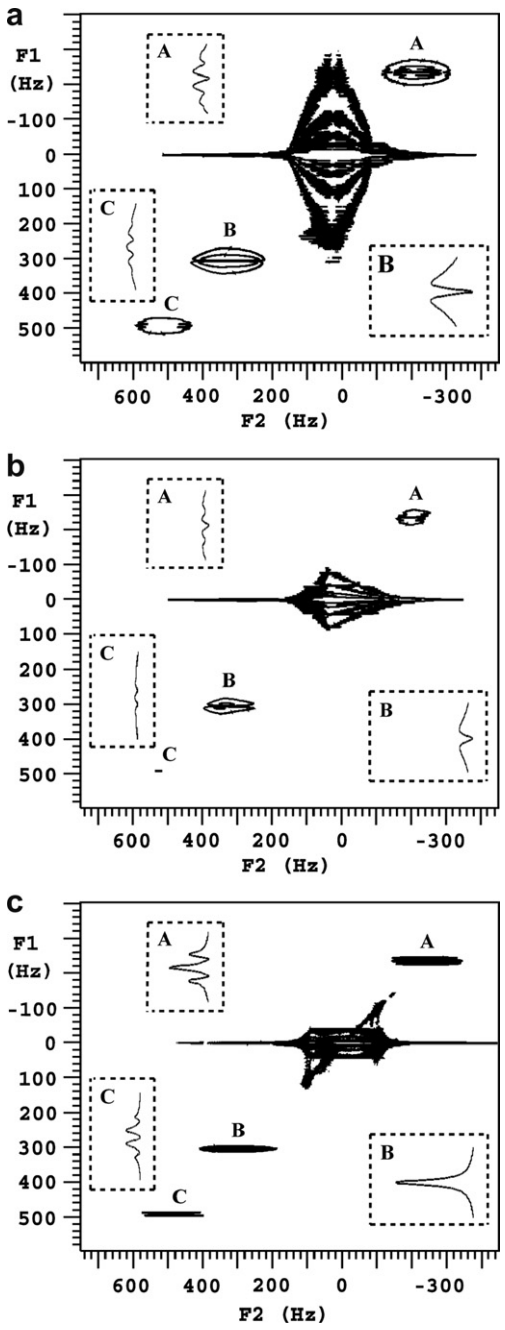

Fig. 6. Experimental 2D iZQC spectra in different kinds of inhomogeneous fields of about 200 Hz in linewidth with a CSG strength $G = 0.03$ T/m. (a) Linear along the *XY* plane, (b) non-linear along the *XY* plane, and (c) linear along the *Z* axis. A four-step phase cycling was applied. The regions of the solute peaks were expanded.

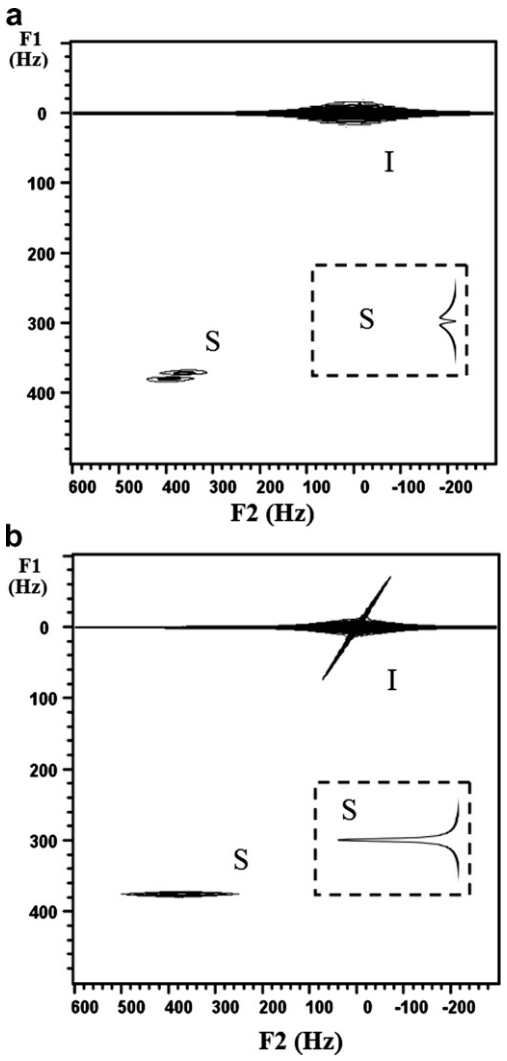

Fig. 7. Simulated iZQC high-resolution spectra under different kinds of inhomogeneous fields with 200 Hz linewidth with a CSG strength $G = 0.03$ T/m. (a) Linear along the *XY* plane, and (b) linear along the *Z* axis. A four-step phase cycling was applied. The regions of the solute peaks were expanded.

Table 1
Evolution time t_1 for the magic angle gradient condition of magnetization modulation at different CSG strengths

G (T/m)		0.01	0.03	0.05	0.07	0.09
t_1(ms)	Theory	11.4	36.8	61.8	87.5	112.8
	Simulation	13.0	37.0	63.0	89.0	>112

The non-monotonic variation of linewidth and signal intensity as shown in Figs. 4 and 5a when the inhomogeneous field is along the *XY* plane can be explained as follows, taking the case of linear inhomogeneous field as an example. Since the inhomogeneous linewidth is about 200 Hz and the inner diameter of the sample tube is about 3.5 mm, the background field gradient is calculated to be $g \approx 1.35 \times 10^{-3}$ T/m. When the CSG strength G and the evolution time t_1 have the values given in Table 1, the magnetization is modulated under the combined effect of the background gradient and CSG. When the magic angle gradient condition of magnetization modulation is satisfied, it results in null DDF [39,40]. It is noted that the simulation results for the t_1 value in Table 1 correspond to the minimal relative signal intensities in the curves of Fig. 5a, in good agreement with the theoretical predictions. Although the iZQC signal does not disappear totally due to non-ideal setting for the magic angle, it is weakest for such cases, as shown in Fig. 5a. From Table 1, it can be seen that with the increase of the CSG strength, the evolution time needed for producing the magic angle gradient condition increases. When the CSG strength reaches certain level, the iZQC signal will be attenuated greatly by diffusion effect before the magic angle magnetization modulation occurs, in which case the magic angle gradient effect will no longer be obvious. This explains why the linewidth decreases after it reaches a maximum at $G = 0.03$ T/m. It is special when the CSG strength is $G = 0.01$ T/m, because the magic angle magnetization modulation occurs soon after the t_1 starts to

increase, and does not disturb the resolution obviously. Similar analysis can be applied for the non-linear inhomogeneous field. When the inhomogeneous field is along the Z axis, the magic angle gradient effect never occurs since the CSG is also along the Z axis. As shown in Fig. 5b, the signal intensity decreases monotonously with the increase of the evolution time t_1 due to the effects of T_2 and diffusion.

Figs. 6 and 7 indicate that the magic angle magnetization modulation distorts the splitting pattern of peaks, and makes it difficult for spectral analysis. In fact, the worst resolution for CSG strength $G = 0.03 \sim 0.05$ T/m was caused by the distorted splitting pattern (Fig. 4). When the singlet splits to the doublet, the linewidth determined as the half-height width of the whole peak is broadened greatly. Therefore, improper CSG intensity must be avoided to achieve high-resolution NMR spectra under inhomogeneous fields.

On the other hand, it can be seen that some additional peaks appear in the position of solvent peak when a CSG is not applied (Fig. 3). These peaks resulted from imperfect RF pulses. They became much weaker when the CSG strength $G = 0.09$ T/m was used. This is because CSGs help to suppress the extra peaks coming from other coherence transfer pathway, such as the remnant signal from the conventional SQC pathway or iDQC pathway.

For high-resolution spectra in the presence of a large inhomogeneous field, the iZQC signal generated without CSGs may possess some advantages over those acquired with CSGs. Since the signal is from the magnetization modulation induced by the background inhomogeneous field itself, it may reflect heterogeneity of microstructures more directly in the *in vivo* localized high-resolution spectra. Furthermore, the diffusion attenuation due to CSGs is reduced, resulting in higher SNR. This property is highly desired for a more general utilization of DDF-related effects which are often hindered by the inherent poor signal-to-noise [2]. Finally, it makes iZQC experiment feasible on the NMR spectrometer without gradient coils.

5. Conclusion

In this paper, iZQC high-resolution spectra in inhomogeneous fields with and without CSGs were compared. The results show that the CSG may be dispensable if an appropriate phase cycling is applied. The spectral resolution of iMQC high-resolution spectroscopy in an inhomogeneous field may not be determined solely by the inhomogeneity inside the correlation distance corresponding to the applied CSG. The simulation results are coincident with experimental ones. Thus the previous view regarding the roles of the dipolar correlation distance needs some amendment. In addition, the magic angle gradient effect may occur when the intrinsic inhomogeneous field is not along the same direction as the CSG. This magic angle gradient effect may distort the peak splitting pattern and reduce spectral resolution. It should therefore be avoided for obtaining high-resolution NMR spectra in the presence of a large inhomogeneous field.

Acknowledgment

This work was partially supported by the NNSF of China under Grants 10605019, 20573084, and 10575085.

References

[1] J.H. Zhong, Z. Chen, E. Kwok, S. Kennedy, Enhanced sensitivity to molecular diffusion with intermolecular double-quantum coherences: implications and potential applications, Magn. Reson. Imag. 19 (2001) 33–39.
[2] W. Barros, D.F. Gochberg, J.C. Gore, Assessing signal enhancement in distant dipolar field-based sequences, J. Magn. Reson. 189 (2007) 32–37.
[3] W. Barros, J.C. Gore, D.F. Gochberg, Simultaneous measurement of D and T_2 using the distant dipolar field, J. Magn. Reson. 178 (2006) 166–169.
[4] S. Ahn, W.S. Warren, S. Lee, Quantum treatment of intermolecular multiple quantum coherences with intramolecular J coupling in solution NMR, J. Magn. Reson. 128 (1997) 114–129.
[5] W.S. Warren, W. Richter, A.H. Andreotti, B.T. Farmer, Generation of impossible cross-peaks between bulk water and biomolecules in solution NMR, Science 262 (1993) 2005–2009.
[6] S. Lee, W. Richter, S. Vathyam, W.S. Warren, Quantum treatment of the effects of dipole–dipole interactions in liquid nuclear magnetic resonance, J. Chem. Phys. 105 (1996) 874–900.
[7] S.S. Velan, P.T. Narasimhan, R.E. Jacobs, MR imaging with phase encoding of intermolecular multiple quantum coherences, J. Magn. Reson. 152 (2001) 189–194.
[8] Z. Chen, Z.W. Chen, J.H. Zhong, Observation and characterization of intermolecular homonuclear single-quantum coherences in liquid nuclear magnetic resonance, J. Chem. Phys. 117 (2002) 8426–8435.
[9] Z. Chen, Z.W. Chen, J.H. Zhong, Quantitative study of longitudinal relaxation related to intermolecular dipolar interactions in solution NMR, Chem. Phys. Lett. 333 (2001) 126–132.
[10] L.S. Bouchard, R.R. Rizi, W.S. Warren, Magnetization structure contrast based on intermolecular multiple-quantum coherences, Magn. Reson. Med. 48 (2002) 973–979.
[11] X.P. Tang, H. Ong, K. Shannon, W.S. Warren, Simultaneous acquisition of multiple orders of intermolecular multiple-quantum coherence images, Magn. Reson. Imag. 21 (2003) 1141–1149.
[12] L.S. Bouchard, W.S. Warren, Multiple-quantum vector field imaging by magnetic resonance, J. Magn. Reson. 177 (2005) 9–21.
[13] Y.Y. Lin, S. Ahn, N. Murali, W. Brey, C.R. Bowers, W.S. Warren, High-resolution >1 GHz NMR in unstable magnetic fields, Phys. Rev. Lett. 85 (2000) 3732–3735.
[14] A. Schäfer, H.E. Möller, Functional contrast based on intermolecular double-quantum coherences: influence of the correlation distance, Magn. Reson. Med. 58 (2007) 696–704.
[15] C. Faber, E. Pracht, A. Haase, Resolution enhancement in *in vivo* NMR spectroscopy: detection of intermolecular zero-quantum coherences, J. Magn. Reson. 161 (2003) 265–274.
[16] P.T. Narasimhan, R.E. Jacobs, Microscopy in magnetic resonance imaging, Annu. Rep. NMR Spectrosc. 55 (2005) 259–297.
[17] R.A. de Graaf, D.L. Rothman, K.L. Behar, High resolution NMR spectroscopy of rat brain *in vivo* through indirect zero-quantum-coherence detection, J. Magn. Reson. 187 (2007) 320–326.
[18] K.M. Koch, P.B. Brown, D.L. Rothman, R.A. de Graaf, Sample-specific diamagnetic and paramagnetic passive shimming, J. Magn. Reson. 182 (2006) 66–74.
[19] J. Shen, D.L. Rothman, Fast automatic adjustment of on-axis shims for high-resolution NMR, J. Magn. Reson. 127 (1997) 229–232.
[20] J. Perlo, F. Casanova, B. Blümich, *Ex situ* NMR in highly homogeneous fields: ^{1}H spectroscopy, Science 315 (2007) 1110–1112.
[21] J. Perlo, V. Demas, F. Casanova, C.A. Meriles, J. Reimer, A. Pines, B. Blümich, High-resolution NMR spectroscopy with a portable single-sided sensor, Science 308 (2005) 1279.
[22] Z. Chen, Z.W. Chen, J.H. Zhong, High-resolution NMR spectra in inhomogeneous fields via IDEAL (Intermolecular Dipolar-interaction Enhanced All Lines) method, J. Am. Chem. Soc. 126 (2004) 446–447.
[23] G. Galiana, R.T. Branca, W.S. Warren, Ultrafast intermolecular zero quantum spectroscopy, J. Am. Chem. Soc. 127 (2005) 17574–17575.
[24] X. Zhu, S. Chen, Z. Chen, S.H. Cai, J.H. Zhong, Simultaneous acquisition and effective separation of intermolecular multiple-quantum signals of different orders, Chem. Phys. Lett. 438 (2007) 308–314.
[25] Y.Q. Lin, Z. Chen, S.H. Cai, J.H. Zhong, Accurate measurements of small J coupling constants under inhomogeneous fields via intermolecular multiple-quantum coherences, J. Magn. Reson. 190 (2008) 298–306.
[26] S. Vathyam, S. Lee, W.S. Warren, Homogeneous NMR spectra in inhomogeneous fields, Science 272 (1996) 92–96.
[27] C. Faber, Solvent-localized NMR spectroscopy using the distant dipolar field: a method for NMR separations with a single gradient, J. Magn. Reson. 176 (2005) 120–124.
[28] S. Garrett-Roe, W.S. Warren, Numerical studies of intermolecular multiple quantum coherences: high-resolution NMR in inhomogeneous fields and contrast enhancement in MRI, J. Magn. Reson. 46 (2000) 1–13.
[29] S. Datta, S.Y. Huang, Y.Y. Lin, Understanding spin turbulence in solution magnetic resonance through phase space dynamics and instability, Concept Magn. Reson. A 28 (2006) 410–421.
[30] Y.Y. Lin, N. Lisitza, S.D. Ahn, W.S. Warren, Resurrection of crushed magnetization and chaotic dynamics in solution NMR spectroscopy, Science 290 (2000) 118–121.
[31] R. Bowtell, P. Robyr, Structural investigations with the dipolar demagnetizing field in solution NMR, Phys. Rev. Lett. 24 (1996) 4971–4974.
[32] G. Deville, M. Bernier, J.M. Delrieux, NMR multiple echoes observed in solid ^{3}He, Phys. Rev. B 19 (1979) 5666–5689.
[33] R. Bowtell, R.M. Bowley, P. Glover, Multiple echoes in a liquid in a high magnetic field, J. Magn. Reson. 88 (1990) 643–651.

[34] J. Jeener, A. Vlassenbroek, P. Broekaert, Unified derivation of the dipolar field and relaxation terms in the Bloch–Redfield equations of liquid NMR, J. Chem. Phys. 103 (1995) 1309–1332.
[35] T. Enss, S. Ahn, W.S. Warren, Visualizing the dipolar field in solution NMR and MR imaging: three-dimensional structure simulations, Chem. Phys. Lett. 305 (1999) 101–108.
[36] C.B. Cai, Z. Chen, S.H. Cai, J.H. Zhong, A simulation algorithm based on Bloch equations and product operator matrix: application to dipolar and scalar couplings, J. Magn. Reson. 172 (2005) 242–253.
[37] C.B. Cai, M.J. Lin, Z. Chen, X. Chen, S.H. Cai, J.H. Zhong, SPROM—an efficient program for NMR/MRI simulations of inter- and intra-molecular multiple quantum coherences, C.R. Physique 9 (2008) 119–126.
[38] Y. Zhao, A.W. Anderson, J.C. Gore, Computer simulation studies of the effects of dynamic shimming on susceptibility artifacts in EPI at high field, J. Magn. Reson. 173 (2005) 10–22.
[39] J.P. Marques, R. Bowtell, Optimizing the sequence parameters for double-quantum CRAZED imaging, Magn. Reson. Med. 51 (2004) 148–157.
[40] G. Lippens, J. Jeener, The dipolar interaction under all angles, Concept Magn. Reson. 13 (2001) 8–18.